

Retrobiosynthetic analysis of carbon fixation in the phototrophic eubacterium *Chloroflexus aurantiacus*

Wolfgang EISENREICH¹, Gerhard STRAUSS², Udo WERZ³, Georg FUCHS² and Adelbert BACHER¹

¹ Lehrstuhl für Organische Chemie und Biochemie, Technical University of Munich, Germany

² Abteilung Angewandte Mikrobiologie, University of Ulm, Germany

³ Abteilung Organische Chemie I, University of Ulm, Germany

(Received (March 9/April 22, 1993) – EJB 93 0349/6)

The phototrophic bacterium *Chloroflexus aurantiacus* does not use any of the known autotrophic CO₂ fixation pathways. There is evidence for a new cyclic autotrophic pathway in which acetyl-CoA is converted to 3-hydroxypropionate and further to succinate and malate. This hypothesis was tested by feeding growing cultures during several generations with 3-hydroxy[1-¹³C]propionate, [1-¹³C]acetate, or [2-¹³C]acetate, in addition to unlabeled CO₂. The relative ¹³C content of individual carbon atoms in biosynthetic amino acids and nucleosides was determined by ¹H- and ¹³C-NMR spectroscopy. ¹³C coupling patterns were analyzed by two-dimensional ¹³C-TOCSY experiments which were optimized for the analysis of multiply ¹³C-labeled biosynthetic samples. From the ¹³C enrichments of amino acids and nucleosides, the labeling patterns of central metabolic intermediates were evaluated by a retrobiosynthetic approach. Both 3-hydroxypropionate and acetate were incorporated into all central metabolic pools. The ¹³C labeling and coupling patterns suggest a novel carbon fixation pathway via 3-hydroxypropionate. Specifically, we propose that acetyl-CoA is carboxylated to malonyl-CoA which is reduced under formation of 3-hydroxypropionyl-CoA. Dehydration and reduction yield propionyl-CoA which is converted to succinate by a second carboxylation reaction. The net product of autotrophic carbon fixation appears to be glyoxylate. However, it is not yet known how glyoxylate is channeled into anabolic metabolism. Assimilation of acetate can proceed via the CO₂ fixation pathway, but also via the glyoxylate pathway.

In bacteria, three pathways of autotrophic CO₂ fixation have been evaluated: the reductive pentose phosphate cycle (Calvin cycle) found in aerobic eubacteria, the reductive citric acid cycle, and the reductive acetyl-CoA/carbon monoxide dehydrogenase pathway found in anaerobic eubacteria and archaeobacteria [1].

Evidence for a fourth autotrophic CO₂ fixation pathway has recently been presented for *Chloroflexus aurantiacus* [2, 3], an anaerobic thermophilic phototrophic eubacterium [4, 5]. This organism excretes substantial concentrations (5 mM) of 3-hydroxypropionate at the end of autotrophic growth on CO₂ plus H₂ [2]; this proves that the bacterium is able to synthesize 3-hydroxypropionate from CO₂ and H₂ alone. The question is whether 3-hydroxypropionate is a dead-end product formed from CO₂ in a side path (e.g. by a peculiar fermentation of storage polyglucose during light limitation in the late growth stage) or whether it is a true intermediate of the novel autotrophic carbon cycle which has not yet been investigated in detail. In the first case, exogenous 3-hydroxy-

propionate should act as a limited biosynthetic precursor, if at all; in the second case, it should act as precursor for all cellular compounds.

It has been proposed that 3-hydroxypropionate is formed via carboxylation of acetyl-CoA and subsequent reduction of the carboxylation product, malonyl-CoA [2]. 3-Hydroxypropionate may be further reduced to propionate which may be converted to succinate by carboxylation. If this hypothesis is correct, 3-hydroxypropionate should serve as precursor for all cell compounds. In order to test this hypothesis we synthesized 3-hydroxy[1-¹³C]propionate and fed it to growing cultures during several generations. Similarly, cells were long-term labeled with [1-¹³C]acetate or [2-¹³C]acetate in order to follow the metabolic fate of acetyl-CoA which is also thought to be an intermediate in the autotrophic cycle. The relative ¹³C enrichment of the individual carbon atoms in amino acids and nucleosides was determined by ¹³C NMR and ¹H-NMR spectroscopy. Coupling between ¹³C was analyzed by two-dimensional ¹³C total correlation spectroscopy (TOCSY).

Traditionally, isotope incorporation studies are interpreted in the forward metabolic direction. In this case, the essential question is whether a given precursor can or can not serve as a precursor for the down-stream product of interest. A different approach was used in the present study. The fed ¹³C-labeled compounds were incorporated into all amino acids and nucleosides leading to complex ¹³C-labeling and

Correspondence to A. Bacher, Lehrstuhl für Organische Chemie und Biochemie, Technische Universität München, Lichtenbergstrasse 4, W-8046 Garching, Germany.

Fax: +49 089 3209 3363

Abbreviations. TPPI, time proportional phase increment; INADEQUATE, incredible natural abundance double quantum transfer experiment; TOCSY, total correlation spectroscopy; MLEV, Malcolm Levitt pulse sequence for decoupling

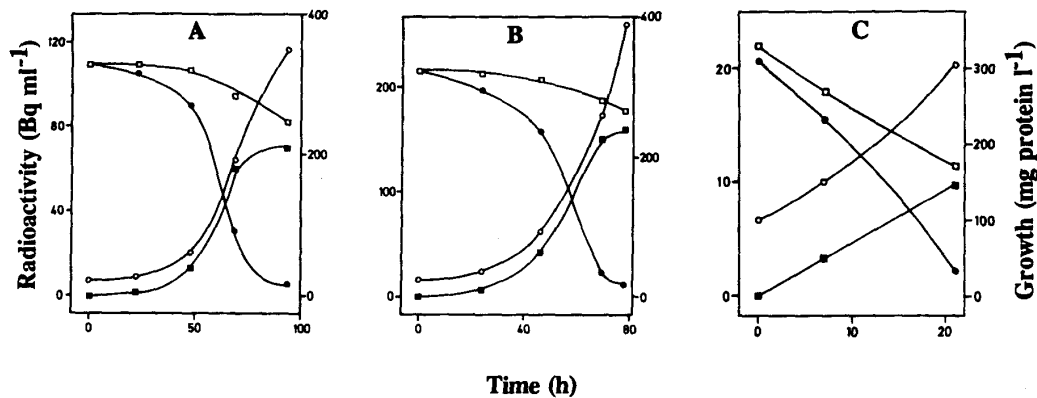


Fig. 1. Growth of *C. aurantiacus* with CO_2 and additional carbon sources. (A) Supplemented with 10 mM $[1\text{-}^{13}\text{C}]$ acetate (99% enrichment) and tracer amounts of $[U\text{-}^{14}\text{C}]$ acetate ($100 \text{ kBq} \cdot \text{l}^{-1}$). (B) Supplemented with 10 mM $[2\text{-}^{13}\text{C}]$ acetate (99% enrichment) and tracer amounts of $[U\text{-}^{14}\text{C}]$ acetate ($100 \text{ kBq} \cdot \text{l}^{-1}$). (C) supplemented with 1 mM 3-hydroxy $[1\text{-}^{13}\text{C}]$ propionate (99% enrichment), 4 mM unlabeled 3-hydroxypropionate and tracer amounts of 3-hydroxy $[1\text{-}^{14}\text{C}]$ propionate ($20 \text{ kBq} \cdot \text{l}^{-1}$). Cell harvest was immediately after the last time point of these experiments. (○) Growth; (■) ^{14}C in washed cells; (●) ^{14}C in cell-free culture supernatant (including $^{14}\text{CO}_2$).

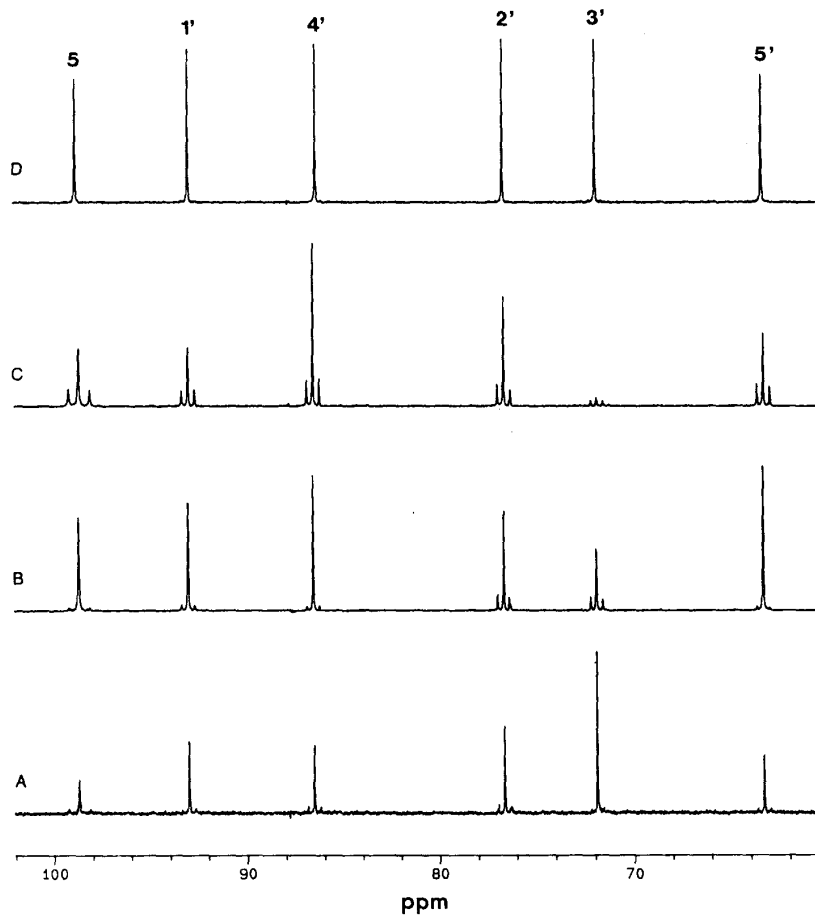


Fig. 2. Partial ^{13}C -NMR spectra of cytidine. (A) sample from growth experiment with 3-hydroxy $[1\text{-}^{13}\text{C}]$ propionate. (B) sample from growth experiment with $[1\text{-}^{13}\text{C}]$ acetate. (C) sample from growth experiment with $[2\text{-}^{13}\text{C}]$ acetate. (D) sample with natural ^{13}C abundance.

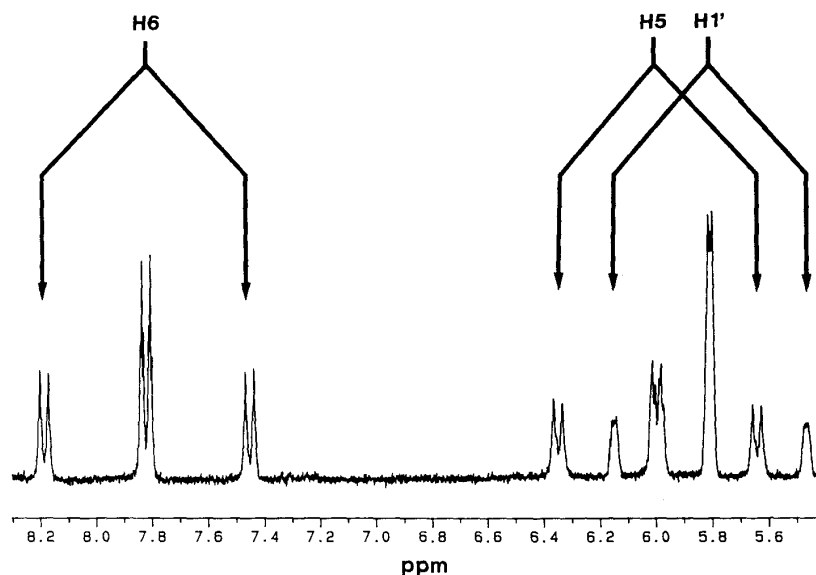


Fig. 3. Partial ^1H -NMR spectrum of cytidine from growth experiment with $[2\text{-}^{13}\text{C}]\text{acetate}$. Satellite signals from coupling with ^{13}C are indicated by arrows.

coupling patterns. Using these data and available knowledge on the pathways of amino acid and nucleoside biosynthesis, the ^{13}C -labeling and coupling patterns of central metabolic pools, such as trioses and dicarboxylic acids, could be deduced with considerable accuracy. These data confirm the proposed role of 3-hydroxypropionate as an intermediate in the novel carbon fixation cycle.

MATERIALS AND METHODS

Organism

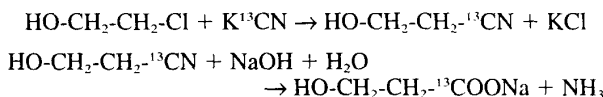
Chloroflexus aurantiacus (DSM 636) was obtained from the *Deutsche Sammlung von Mikroorganismen* (Braunschweig, Germany). Growth conditions and media have been described earlier [3]. Briefly, *C. aurantiacus* was grown under anaerobic conditions under gassing with H_2/CO_2 (80/20, by vol.). The sodium salts of $[1\text{-}^{13}\text{C}]\text{acetate}$, $[2\text{-}^{13}\text{C}]\text{acetate}$ (99% ^{13}C), or 3-hydroxy $[1\text{-}^{13}\text{C}]\text{propionate}$ (20% ^{13}C) were added as sterile solutions to a final concentration of 10 mM acetate or 5 mM 3-hydroxypropionate, respectively, when the cell density had reached a value of 30–100 mg protein \cdot l $^{-1}$. In addition, 100–200 kBq of filter-sterilized 3-hydroxy $[1\text{-}^{14}\text{C}]\text{propionate}$ or $[\text{U}\text{-}^{14}\text{C}]\text{acetate}$ was added/l in order to monitor 3-hydroxypropionate and acetate metabolism and to facilitate the isolation of cellular components. Samples were retrieved at intervals to determine growth and the ^{14}C content of cells and supernatant. Cell growth was continued as indicated in Fig. 1. Cells were harvested aerobically by centrifugation. 3-Hydroxypropionate and succinate were determined in the medium of *C. aurantiacus* by gas chromatography.

Chemicals

$[^{14}\text{C}]\text{KCN}$ was from Amersham Buchler (Braunschweig, Germany). $[^{13}\text{C}]\text{KCN}$, $[1\text{-}^{13}\text{C}]\text{acetate}$ and $[2\text{-}^{13}\text{C}]\text{acetate}$ were from MSD-Isotopes (IC-Chemikalien, München, Germany). Gases were purchased from Linde (Höllriegelskreuth, Germany).

Synthesis of 3-hydroxy $[1\text{-}^{13}\text{C}]\text{propionate}$

The compound was prepared by the following sequence of reactions [6, 7]:



A small amount of K^{14}CN (185 kBq) was added to the reaction mixture containing 5 g K^{13}CN .

Derivatization of isolated amino acids

Isolated amino acid (0.14 nmol) and sodium bicarbonate (1.4 nmol) were dissolved in 1 ml water. Benzoyl chloride (0.4 mmol) was added in small portions and the reaction mixture was stirred at room temperature for 45 min. The mixture was then adjusted to pH 3 by the addition of 2 M hydrochloric acid and was kept at 4 °C overnight. The residue was removed by filtration, and the filtrate was purified by preparative HPLC on a column of Lichrosorb RP_{18} (16 \times 250 mm; eluent, 100 mM formic acid in 30% methanol; flow, 10 ml/min). The effluent was monitored photometrically (280 nm). Fractions were pooled and evaporated to dryness under reduced pressure.

NMR Spectroscopy

^1H - and ^{13}C -NMR spectra were recorded at 360 MHz and 90.6 MHz, respectively, with a Bruker AM 360 NMR spectrometer equipped with fast power switching of the transmitter output (Fast-TLO) and with an external pulse amplifier (BFX5, Bruker).

^1H -NMR spectra were measured as follows: 50° pulse (4 μs); repetition time, 2.5 s; spectral width, 5.3 kHz; 16 000 data set; temperature, 25 °C; 0.2 Hz line broadening. ^{13}C -NMR spectra were measured as follows: 30° pulse (2 μs); repetition time, 2.8 s; spectral width, 20.8 kHz, 32 000 data

Table 1. Relative ^{13}C enrichments in amino acids and nucleosides isolated from cells of *C. aurantiacus* grown for several generations with CO_2 (natural ^{13}C abundance) in the presence of 5 mM 3-hydroxy[1- ^{13}C]propionate (20% ^{13}C enrichment), or 10 mM [1- ^{13}C]acetate (99% ^{13}C enrichment), or 10 mM [2- ^{13}C]acetate (99% ^{13}C enrichment). ^{13}C enrichments obtained from ^1H -NMR spectra are marked by asterisks. $^1J_{\text{cc}}$ values were obtained from one-dimensional ^{13}C -NMR spectra. The percentage coupling is the fraction of ^{13}C - ^{13}C coupled satellites; carbon atoms involved in ^{13}C coupling are indicated in brackets. n.d., not determined; r = ring.

Metabolite	Carbon position	Chemical shift	$^1J_{\text{cc}}$	Growth with				
				3-hydroxy-[1- ^{13}C]-propionate ^{13}C	[1- ^{13}C]acetate		[2- ^{13}C]acetate	
		ppm	Hz	%	^{13}C	coupling	^{13}C	coupling
Alanine	1	175.3	59.5	8.0	10.2		4.6	47.8(2)
	2	51.4	59.5	1.2	16.3*		52.3	3.1 (1) 25.1 (3)
	3	18.0	34.0	1.6*	22.4*	3.1 (2)	38.5*	39.0 (2)
Threonine	1	172.8	59.6	5.2	8.0		4.2	40.0 (2)
	2	61.0	36.2	1.4	26.1		42.1	40.5 (3)
	3	67.9	36.3	1.4	21.9		48.4	39.9 (2)
	4	21.7	38.0	4.4*	19.8*		2.3*	47.3 (3)
Aspartic acid	1	185.0	53.7	3.9	13.7		2.1	42.8 (2)
	2	56.6	35.6	1.7*	20.5*	5.4 (3)	44.7	38.9 (3)
			53.5			3.4 (1)		
	3	45.9	35.6	1.7*	19.1	5.2 (2)	47.6*	39.1 (2) 1.7 (4)
		51.1			2.1 (4)			
4	182.9	51.5	4.8	17.7		2.5	44.0 (3)	
Glutamic acid	1	176.2	54.9	6.8	15.9	2.5 (2)	3.3	45.4 (2)
	2	56.3	37.7	2.2*	20.6*	7.3 (3)	52.8*	42.0 (3)
			54.2			2.9 (1)		2.1 (1)
	3	28.0	35.4	2.2	21.5	15.8 (4,2)	54.3	
	4	32.5	35.7	2.2	9.4	18.1 (3)	80.8	55.9 (3) 2.0 (5)
		54.6			5.3 (5)			
5	179.5	54.2	6.6	43.0	2.3 (4)	3.0	40.0 (5)	
Proline	1	174.2		n.d.	n.d.		n.d.	
	2	62.0	31.9		17.7		55.8*	43.5 (3)
	3	30.8	30.3		21.9	17.3 (4,2)	67.7	74.3 (4,4)
	4	25.9	30.9		8.4	27.3 (3,5)	93.7	57.4 (3,5)
	5	48.8	33.4		59.9*		2.7	48.1 (4)
Arginine	1	174.2		n.d.	18.6		n.d.	
	2	55.2	33.8		21.5		56.6*	37.8(3)
	3	29.7	33.7		21.4	14.9 (2,4)	53.2	74.8 (2,4)
	4	26.4	34.7		7.7	23.4 (3,5)	79.0	58.1 (3,5)
	5	43.0	36.4		53.4*		2.4	45.8 (4)
	6	159.4			0.7		1.1	
Methionine	1	174.3		n.d.	19.9		n.d.	
	2	54.4			22.8		n.d.	
	3	31.5			19.2		n.d.	
	4	31.2			18.8		n.d.	
	5	16.6			24.0*		45.5*	
Lysine	1	174.3	59.2	n.d.	59.3		3.4	38.2 (2)
	2	54.8	33.1		n.d.		71.7*	55.9 (3)
	3	31.8	33.4		21.1	15.2 (2,4)	46.3	71.9 (2,4)
	4	24.0	34.4		22.0	13.2 (3,5)	36.3	75.9 (3,5)
	5	28.8	34.3		8.0	27.5 (4,6)	74.7	57.9 (4,6)
	6	41.7			56.8*		n.d.	
Valine	1	174.0		n.d.	19.5		n.d.	
	2	60.8	32.6		13.9	12.2 (3)	54.7*	60.5 (3)
	3	31.5	34.7		15.3	56.8 (2,4,5)	57.4	73.3 (2,4,5)
	4	19.9	34.6		26.5*	3.0 (3)	46.3	37.6 (3)
	5	19.4	34.5		26.5*	21.1 (3)	43.3	58.9 (3)

Table 1. (continued).

Metabolite	Carbon position	Chemical shift	$^1J_{cc}$	Growth with				
				3-hydroxy-[1- ^{13}C]-propionate ^{13}C	[1- ^{13}C]acetate		[2- ^{13}C]acetate	
					^{13}C	coupling	^{13}C	coupling
		ppm	Hz	%				
Leucine	1	175.2	59.2	4.0	55.9		3.0	60.0 (2)
	2	54.2	33.2	2.0	6.8	25.0 (3)	72.3	61.1 (3)
			60.8			11.7 (1)		
	3	41.5	33.3	1.7	19.1	29.8 (2,4)	47.3	67.2 (2,4)
	4	26.6	34.6	1.8	19.8	59.1 (3,5,6)	51.2	75.2 (3,5,6)
	5	24.3	34.8	2.1	29.9		35.6*	38.8 (4)
6	23.6	35.0	2.0*	29.3*		35.6*	60.9 (4)	
Isoleucine	1	174.1		n.d.	21.6		n.d.	
	2	59.9	32.6		21.6	25.0 (3)	48.8	61.3 (3)
	3	38.4	33.4, 30.1		21.6	29.2 (2,4,6)	58.1	74.2 (2,4,6)
	4	27.5	34.3		25.9	25.1 (3,5)	55.6	60.4 (3,5)
	5	16.8	34.7		23.7	4.0 (4)	8.1	40.7 (4)
	6	13.6	34.8		30.2*	4.0 (3)	40.9*	36.7 (3)
Phenylalanine	1	173.7		n.d.	19.1		n.d.	
	2	56.5			24.1*		58.1*	
	3	38.0	43.5		31.6	24.4(r-1)	35.0	
	r-1	136.4	56.6, 43.9		22.8	44.3(r-2/6,3)	57.3	
	r-2/6,-3/5	131.9		25.8 ^a		31.4 ^a		
r-4	130.6			19.1		7.8		
Tyrosine	1	185.6	53.2	3.4	10.4	5.7 (2)	5.2	42.3 (2)
	2	60.2	33.1	1.4*	19.7	3.5 (3)	51.6	23.6 (3)
			53.1			2.5 (1)		3.1 (1)
	3	42.5	45.6, 35.2	1.8	29.0	27.6(r-1,2)	40.8	63.2(r-1,2)
	r-1	126.3	56.6, 46.6	1.1	15.5	50.9(r-2/6,3)	45.0	61.5(r-2/6,3)
	r-2/6	133.3	56.2	1.7	28.0*	26.1(r-3/5,r-1)	39.0*	56.1(r-3/5,r-1)
	r-3/5	121.2	60.4, 56.4	2.8	19.7	26.9(r-2/6,r-4)	38.3	34.5(r-2/6,r-4)
r-4	167.2	61.0	3.7	11.4	26.3(r-3/5)	4.6	45.6(r-3/5)	
Guanosine	2	153.7		3.4	27.4		n.d.	
	4	151.3		4.6	14.9			
	5	116.7		n.d.	21.1			
	6	156.8		1.0	1.0			
	8	135.6		2.3*	30.8*			
	1'	86.3		2.0	22.0*			
	2'	73.7	37.5	1.8	17.9	26.9(1',3')		
	3'	70.4	37.8	5.1	12.7	27.0(2',4')		
	4'	85.2		1.6	18.4			
	5'	61.4		1.7	22.4			
Cytidine	2	160.1		0.9	n.d.		n.d.	
	4	168.6		3.0	17.0		1.0	
	5	98.7	68.4	2.4	23.2*		52.3*	39.0 (6)
	6	144.1	68.3	2.1	23.2*		49.4*	38.4 (5)
	1'	92.9	42.9	2.7*	21.0*		31.4*	37.9 (2')
	2'	76.6	42.6	3.1	18.0		44.0	30.5 (1',3')
	3'	71.8	37.9	4.7	13.4		7.0	54.2 (2',4')
	4'	86.3	41.8	2.6	18.1		54.8	30.4 (3',5')
5'	63.3	42.0	2.2	23.9		36.9	37.7 (4')	
Adenosine	2	154.6		4.9	22.3		37.7	
	4	150.6		4.6	10.5		n.d.	
	5	121.3		n.d.	30.7		58.3	
	6	157.8		n.d.	n.d.		n.d.	
	8	142.8		3.8	23.6		37.1	
	1'	90.4	42.7	3.0	15.5*		29.4*	34.4 (2')
	2'	75.7	42.6	2.8	12.0	19.6 (1',3')	36.0	29.1 (1',3')
	3'	72.7	37.9	6.5*	7.0	22.6 (2',4')	6.8	56.4(2',4')
	4'	87.9	40.6	1.4	13.0		43.3	28.9 (3',5')
	5'	63.6	41.1	2.3	13.5		26.2	37.2 (4')

^a Averaged due to signal overlapping.

set zero-filled to 64 000; temperature, 25°C; ¹H composite pulse decoupling; 1 Hz line broadening.

Two-dimensional ¹³C TOCSY experiments were performed with the MLEV-17-based two-dimensional magnetization transfer procedure [8]. The ¹³C-excitation pulse was generated in the transmitter high power output level (THI; 90° pulse, 5 μs). ¹³C-mixing pulses were generated in the transmitter low power output level amplified with a BFX5 unit (TLO; 90° pulse, 50 μs). The MLEV-17 mixing period was 60 ms and was preceded and followed by 2.5-ms trim pulses. The data were acquired in the phase-sensitive mode using time proportional phase increments (TPPI). Other data acquisition and processing parameters were as follows: 32 scans per *t*₁ increment; 2.0 s relaxation delay; 400 × 2048 raw data matrix size zero-filled to 2048 in *t*₁, and processed with 45° shifted squared sine bell functions in *t*₁ and *t*₂.

Alanine, threonine, proline, methionine, valine, leucine, isoleucine, arginine, and phenylalanine were measured in D₂O/NaOD (pH 13), aspartic acid and tyrosine in 0.1 M NaOD, adenosine, cytidine and glutamic acid in D₂O (pH 5), and guanosine in (D₆)dimethylsulfoxide. Signal assignments have been reported earlier [9].

RESULTS

Growth experiments

Chloroflexus aurantiacus was grown anaerobically in 1 l on pure mineral medium under an atmosphere of H₂/CO₂ (4/1, by vol.). When the cell density had reached a protein content of 30–100 mg/l, [1-¹³C]acetate or [2-¹³C]acetate (99% ¹³C) was added to a final concentration of 10 mM. In order to monitor the fate of acetate, a small amount of [U-¹⁴C]acetate was included (Fig. 1A and B). The mean generation time decreased from 32 h under pure autotrophic growth conditions to 17 h. Cells were harvested when approximately 95% of ¹⁴C had disappeared from the culture medium. Approximately 65% of the radiolabel from acetate were incorporated into cell material, and 17% of label was lost, probably as ¹⁴CO₂. Acetate contributed 14 mmol carbon/l or 170 mg carbon out of approximately 380 mg cell carbon/l. Thus, about 40% of cell carbon was derived from acetate carbon, and 60% was fixed from CO₂.

Alternatively, *C. aurantiacus* was grown with addition of 5 mM 3-hydroxy[1-¹³C]propionate (20% ¹³C enrichment) and a trace amount of 3-hydroxy[1-¹⁴C]propionate (Fig. 1C). The mean generation time was 13 h. The cells were harvested in the logarithmic growth phase. 45% of proffered ¹⁴C was incorporated into cell material; about 50% of ¹⁴C was lost as ¹⁴CO₂. Hence, 2.2 mmol 3-hydroxypropionate contributed 6.7 mmol of carbon/l or 81 mg carbon to a cell mass of 500 mg dry matter (250 mg carbon/l). It follows that approximately one third of total cell carbon was from 3-hydroxypropionate and two thirds from CO₂.

Amino acids and nucleosides were isolated after hydrolysis of cellular proteins and RNA, and were purified by ion-exchange chromatography and preparative HPLC as described earlier [3, 10].

NMR experiments

¹³C abundance in amino acids and nucleosides from growth experiments of *C. aurantiacus* was analyzed by quantitative NMR spectroscopy [3]. Briefly, ¹³C-NMR spectra of biosynthetic samples and of samples with natural ¹³C abun-

Table 2. ¹³C enrichment of *N*-benzoyl-glutamate synthesized from benzoyl chloride with natural ¹³C abundance and glutamic acid from the growth experiment with [2-¹³C]acetate. The ¹³C-NMR signals at 131.3 and 129.7 ppm (ring carbons 2, 3, 5, and 6) were used as internal reference of 1.1% ¹³C abundance. ¹³C enrichments calculated by analysis of ¹³C-coupled satellite signals in the ¹H-NMR spectrum are in brackets. Bz = benzoyl

Position	δ	¹³ C abundance
	ppm	%
1	179.5	2.6 (3.3)
5	177.7	2.6 (3.0)
Bz carbonyl	173.4	1.0
Bz ring 1	135.4	1.0
Bz ring 4	134.9	1.2
Bz ring 2,3,5,6	131.3	1.1
	129.7	1.1
2	55.0	54.8 (52.8)
4	32.8	76.0 (80.8)
3	28.2	56.4 (54.3)

dance (1.1% ¹³C) were recorded under identical conditions. Relative ¹³C abundance of individual carbon atoms was then calculated from the integrals of ¹³C signals of biosynthetic samples by comparison with the ¹³C integrals of natural abundance samples (Fig. 2). In earlier studies [3] it was found that at least one carbon atom of each metabolite studied was derived from a carbon source with the natural ¹³C abundance of 1.1%. In the present experiments, it became obvious that ¹³C enrichment above the natural abundance level was present in most or all carbon atoms of individual metabolites, and it was therefore not possible to estimate absolute ¹³C enrichment values from the ¹³C NMR spectra alone.

To determine absolute ¹³C abundance, we used two different methods. (a) Quantitative analysis of ¹³C-coupled satellite signals in ¹H-NMR spectra gave absolute ¹³C enrichments for at least one carbon atom of each metabolite under study (Fig. 3). Based on these data, absolute ¹³C abundance for the other carbon atoms was then calculated from the relative ¹³C enrichment values obtained from the ¹³C-NMR integrals (Table 1). This approach requires that at least one ¹³C-coupled satellite signal lies in a non-crowded region of the ¹H-NMR spectrum. (b) The ¹³C-NMR integrals were internally referenced by chemical derivatization of the metabolites under study. Specifically, amino acids were converted to the respective *N*-benzoyl derivatives using benzoyl chloride with natural ¹³C abundance. The ¹³C-NMR integrals of the benzoyl signals were then used as an internal reference of 1.1% ¹³C abundance. As shown in Table 2, both methods yield comparable ¹³C enrichment values.

The present study used singly ¹³C-labeled precursors throughout. However, the initial analysis of the ¹³C spectra revealed the diversion of label to virtually all carbon atoms in some metabolites. This could mean that the metabolites under study were a mixture of molecular species with label in different position. Alternatively, the findings could mean that multiple isotope labels had been contributed to adjacent carbon atoms in a single molecular species.

The presence of ¹³C label in pairs of adjacent carbon atoms is easily detected by ¹³C-¹³C coupling in one-dimensional ¹³C-NMR spectra which allows the quantitative assessment of the double-labeled species (Table 1). Moreover, the presence of double-labeled molecules can be observed by

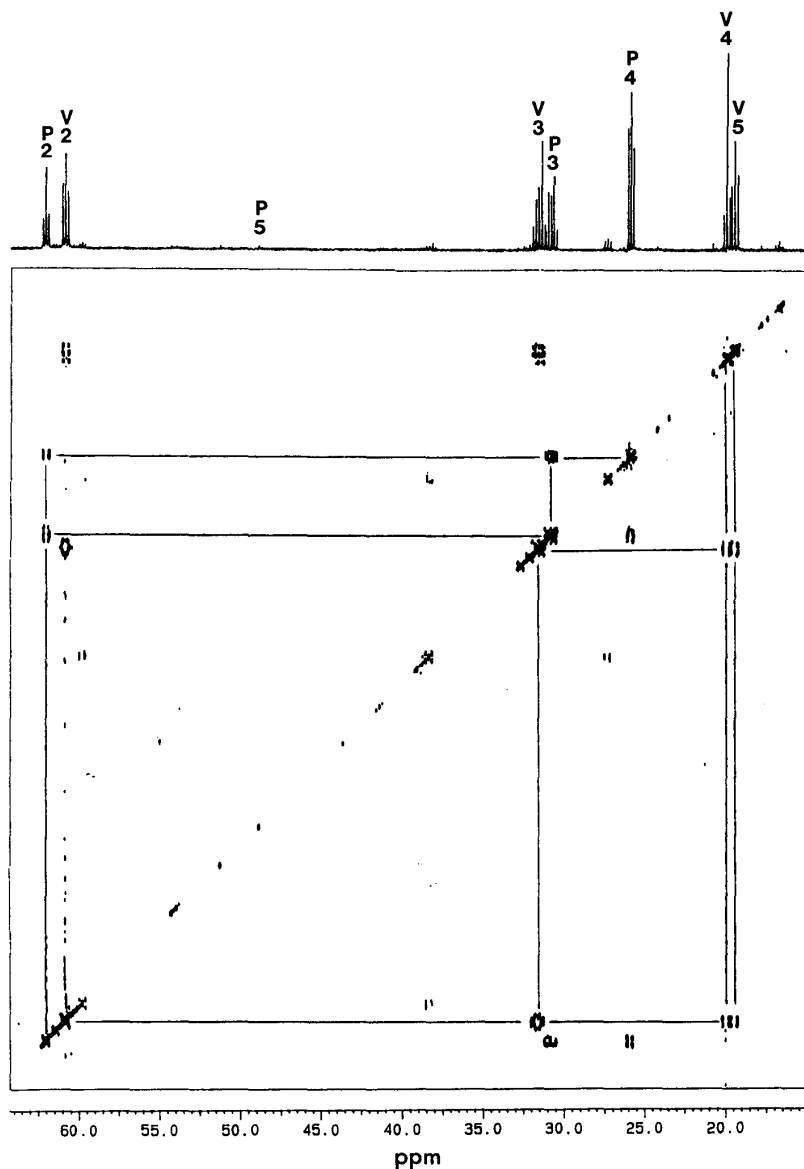


Fig. 4. ^{13}C -TOCSY of a mixture containing proline (P) and valine (V) from the growth experiment with $[2-^{13}\text{C}]$ acetate. ^{13}C spin systems indicating contiguous ^{13}C coupled atoms are connected by lines. The one-dimensional ^{13}C -NMR spectrum of proline and valine from the growth experiment with $[2-^{13}\text{C}]$ acetate is shown at the top of the figure.

INADEQUATE spectroscopy (data not shown). As shown below, metabolites with double labeling in adjacent carbon atoms were indeed generated in appreciable quantity.

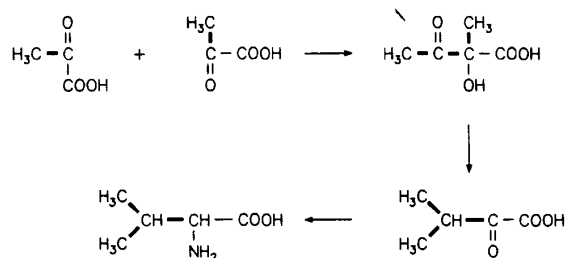
The presence of multiple labeling in three or more contiguous carbon atoms can not be detected by one-dimensional spectroscopy due to the small size of multiple bond ^{13}C - ^{13}C coupling. However, it can be detected by two-dimensional TOCSY spectroscopy which permits the transfer of magnetization along a series of uninterrupted ^{13}C atoms (Fig. 4, Table 3). TOCSY transfer has been used extensively in ^1H spectroscopy [8] and has recently been adapted for studies of totally ^{13}C -labeled proteins [11]. However, the technique has

not been applied previously to the study of biosynthetic problems.

Fig. 4 shows a two-dimensional ^{13}C -TOCSY spectrum of proline and valine from the growth experiment with $[2-^{13}\text{C}]$ acetate. Valine exhibited multiple ^{13}C coupling between C2, C3, C4, and C5 reflecting its formation by standard biosynthetic pathways (Fig. 5). The combination of two ^{13}C -labeled pyruvate molecules leads to multiple ^{13}C coupling in 2-acetolactate. 2-Oxoisovalerate is subsequently formed by methyl migration and is finally transaminated yielding the observed C2/C3/C4/C5 multiple ^{13}C -coupled valine species. ^{13}C coupling between C2, C3, and C4 of proline directly reflects the

Table 3. ^{13}C - ^{13}C -correlation pattern from two-dimensional ^{13}C -TOCSY experiments.

Amino acid	Position	Growth experiment with	
		[1- $^{13}\text{C}_1$]acetate	[2- $^{13}\text{C}_1$]acetate
Proline	2	3	3,4
	3	4	2,4
	4	3	3
	5		
Valine	2	3	3,4,5
	3	2,5	2,4,5
	4		3,2
	5	4	3,2
Leucine	2		3,4,5,6
	3	4	2,4,5,6
	4	3,6	2,3,5,6
	5		2,3,4,6
	6	4	2,3,4,5
Isoleucine	2		3,4,6
	3	4	2,4,6
	4	3	2,3,6
	5		
	6		2,3,4

**Fig. 5.** Biosynthesis and labeling pattern of valine formed in *C. aurantiacus* grown in the presence of [2- ^{13}C]acetate. Bold lines indicate ^{13}C - ^{13}C coupling as shown by two-dimensional ^{13}C -TOCSY experiments (see also Fig. 4).

coupling pattern of its biosynthetic precursor, 2-oxoglutarate, which is discussed below.

Retrobiosynthetic analysis

Labeling patterns of central metabolic intermediates, such as pyruvate, oxaloacetate, and 2-oxoglutarate were deduced by a retrobiosynthetic approach. Previous studies using ^{14}C - and ^{13}C -labeled precursors had indicated that alanine, aspartate and glutamate are conventionally formed by transamination from pyruvate, oxaloacetate, and 2-oxoglutarate, respectively [3]. Therefore, the labeling patterns of pyruvate, oxaloacetate, and 2-oxoglutarate are directly reflected in the labeling patterns of their corresponding transamination products.

Moreover, information on the labeling patterns of the central metabolic intermediates is also reflected by the labeling patterns of various other amino acids and nucleosides on the basis of known biosynthetic pathways. Thus, the labeling pattern of 2-oxoglutarate is not only reflected in glutamate but also in arginine, proline, and lysine, as indicated in Table

1 and Fig. 6. The labeling pattern of pyruvate is reflected in the side chains of aromatic amino acids in line with their formation via chorismate. The labeling pattern of oxaloacetate is reflected in aspartate but also in threonine and methionine via aspartate semialdehyde [12]. Moreover, the labeling of C5 and C6 of cytidine corresponds with C3 and C2 of oxaloacetate, suggesting conventional biosynthesis of pyrimidines via orotate. The labeling patterns of acetyl-CoA and ribose were also reconstructed from known biosynthetic pathways (Fig. 6, Table 4). Since a large number of metabolic products have been analyzed, the labeling patterns of the central intermediates were overdetermined and could thus be obtained with high statistical significance (Tables 4–6). For example, the ^{13}C enrichment of C3 of oxaloacetate based on evaluation of eight metabolites from the growth experiment with [1- ^{13}C]acetate had a value of $21.1 \pm 2.6\%$ (Table 5). Moreover, the data also confirm that the formation of primary metabolites studied proceeds via standard pathways in *C. aurantiacus*.

^{13}C pattern after feeding of [1- ^{13}C]acetate

^{13}C enrichments of metabolites formed during growth with [1- ^{13}C]acetate are shown in Table 5. Labeling patterns of central metabolites deduced from these values are summarized in Fig. 7. If two adjacent carbon atoms show significant labeling in combination with a high level of coupling between them, it can be concluded that a significant amount of double-labeled molecules is present. The presence of double-labeled species is indicated in Fig. 7 by a bold line between the respective carbon atoms.

As expected, C1 of acetyl-CoA showed a high level of enrichment (55%) in the experiment with [1- ^{13}C]acetate. However, a significant amount of label (8%) was also diverted to C2 of acetyl-CoA. There was no evidence for the formation of double-labeled acetyl-CoA.

The labeling of all carbon atoms in pyruvate and oxaloacetate was rather uniform with values ranging over 15–28%. Double-labeled or multiple-labeled molecules were not detected in appreciable amounts. The carbon atoms 1–3 of 2-oxoglutarate were all labeled with enrichment values around 20%.

A significant fraction of 2-oxoglutarate molecules showed evidence for double labeling in C3/C4. This indicates that 2-oxoglutarate was biosynthesized by condensation of two labeled molecules. In line with this observation, we have shown earlier that 2-oxoglutarate is formed by condensation of oxaloacetate and acetyl-CoA, namely by a *si*-stereospecific citrate synthase followed by decarboxylation of isocitrate [3].

^{13}C pattern after feeding of [2- ^{13}C]acetate

The reconstructed labeling patterns of central intermediates in the experiment with [2- ^{13}C]acetate are shown in Table 6 and Fig. 7. The carboxy groups of acetyl-CoA, pyruvate, oxaloacetate, and 2-oxoglutarate had only low levels of ^{13}C enrichment around 3–4%. C2 of acetyl-CoA and C4 of 2-oxoglutarate had about 80% enrichment. All other carbon atoms showed enrichments of 40–50%. Multiple labeling was observed for the following carbon atoms: C2/C3 of pyruvate, C2/C3 of oxaloacetate, and C2/C3/C4 of 2-oxoglutarate. Obviously, the bonds between these carbon atoms had been formed by condensation of ^{13}C -labeled precursors. For formation of the C3/C4 bond of 2-oxoglutarate by condensation

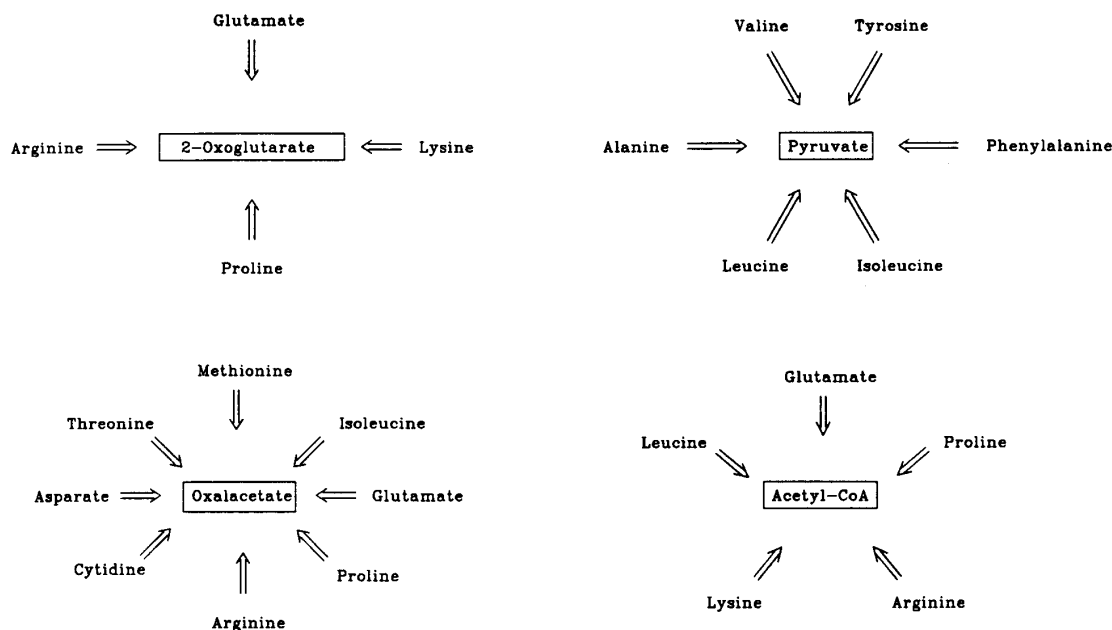


Fig. 6. Reconstruction of ^{13}C enrichment patterns of central metabolites in *C. aurantiacus* by a retrobiosynthetic approach. Starting from ^{13}C enrichments of amino acids and nucleosides, the ^{13}C enrichments of central metabolites were reconstructed by following standard bacterial pathways (for details see Table 4). The symbol \Rightarrow indicates reconstructed precursors in analogy to the retrosynthesis concept in organic chemistry.

of two ^{13}C -labeled fragments had been already shown in the experiment with $[1-^{13}\text{C}]$ acetate.

Labeling pattern after feeding of 3-hydroxy $[1-^{13}\text{C}]$ propionate

All amino acids and nucleosides analyzed showed incorporation of label into at least one carbon atom. Hence, 3-hydroxypropionate is a general metabolic precursor for all metabolites. Labeling of central metabolic pools was calculated as described above and is shown in Table 4 and Fig. 7.

The carboxy groups of acetyl-CoA, pyruvate, oxaloacetate, and 2-oxoglutarate were uniformly labeled with enrichment values around 5–6%. All other carbon atoms showed values around 2% (i.e. about 1% above the natural abundance level).

This experiment was performed with 20% ^{13}C -enriched precursor, whereas the acetate experiments were performed with 99% enriched precursor. For comparison of absolute incorporation rates, the values of the hydroxypropionate experiment should be multiplied by 5. With this in mind, it follows that about one third of cell carbon was generated from fed hydroxypropionate and two thirds from CO_2 . This is well in line with the estimate obtained from the ^{14}C measurements described above. As a consequence of the relatively low enrichments, ^{13}C - ^{13}C coupling was not observed in this experiment.

DISCUSSION

3-Hydroxypropionate is accumulated by *C. aurantiacus* in considerable amounts. Earlier studies [2, 3] had suggested

that the compound is an intermediate in the novel carbon dioxide fixation cycle as shown in Fig. 8. If this hypothesis is correct, label from 3-hydroxypropionate should be diverted to all metabolites. This has now been directly confirmed by the incorporation study with 3-hydroxy $[1-^{13}\text{C}]$ propionate.

The labeling pattern of the 17 metabolites analyzed are all satisfactorily explained by the sequence of reactions shown in Fig. 8. Briefly, it is proposed that the proffered 3-hydroxy $[1-^{13}\text{C}]$ propionate is sequentially converted to $[1/4-^{13}\text{C}]$ succinate via $[1-^{13}\text{C}]$ propionate [2] and $[1-^{13}\text{C}]$ succinyl-CoA. It is further assumed that succinate is converted to $[1/4-^{13}\text{C}]$ malate. Since succinate is a symmetrical molecule, the label can end up in the 1 or 4 position of malate as shown by closed circles in Fig. 8.

Cleavage of malate yields $[1-^{13}\text{C}]$ acetate which can return into the cycle. However, the label will appear in position 3 of hydroxypropionate in the second round. Moreover, the second round can now divert label to position 2 and 3 of malate as indicated by asterisks in Fig. 8.

The net product of CO_2 fixation should be glyoxylate which is generated in the malate cleavage reaction. Malyl-CoA lyase is present in *C. aurantiacus* (unpublished results). However, as discussed in [3], it is not yet known how glyoxylate is diverted into the general metabolism.

Dehydrogenation of malate yields oxaloacetate which can react with acetyl-CoA under formation of citrate. As shown above, acetyl-CoA can be labeled in position 1 (if derived from the first round of CO_2 fixation) or in position 2 (if derived from a subsequent round in the cycle). Citrate can then yield 2-oxoglutarate by the reactions shown in Fig. 8. In line with these predictions, 2-oxoglutarate shows relatively high labeling in both carboxyl groups and low, but significant labeling in all other carbon atoms.

Table 4. Averaged ^{13}C enrichments of central metabolic pools in *C. aurantiacus* grown with [3-hydroxy- ^{13}C]propionate. The ^{13}C enrichments were deduced by a retrobiosynthetic approach from ^{13}C enrichments of amino acids and nucleosides. ^{13}C abundance of acetyl-CoA was calculated from C5 (Glu,Pro,Arg), C6 (Lys), C1 (Leu,-Lys) = C1 (acetyl-CoA); C4 (Glu,Pro,Arg), C5 (Lys), C2 (Leu,-Lys) = C2 (acetyl-CoA). ^{13}C abundance of pyruvate/phosphoenolpyruvate was calculated from C1 (Ala,Val,Tyr,Phe) = C1 (pyruvate); C2 (Ala,Val,Tyr,Phe), C3 (Leu,Ile,Val), C4 (Leu), ring C1 (Tyr,Phe) = C2 (pyruvate); C3 (Ala,Tyr,Phe), C4 (Val), C5 (Leu,-Val), C6 (Leu,Ile) = C3 (pyruvate). ^{13}C abundance of oxaloacetate was calculated from C1 (Asp,Thr,Met,Ile) = C1 (oxaloacetate); C2 (Asp,Thr,Met,Ile), C3 (Glu,Pro,Arg), C6 (Cyt) = C2 (oxaloacetate); C3 (Asp,Thr,Met), C2 (Glu,Pro,Arg), C4 (Ile), C5 (Cyt) = C3 (oxaloacetate); C4 (Asp,Thr,Met), C1 (Glu,Pro,Arg), C5 (Ile) = C4 (oxaloacetate). ^{13}C abundance of 2-oxoglutarate was calculated from C1 (Glu,Pro,Arg) = C1 (oxoglutarate); C2 (Glu,Arg,Pro); C3 (Lys) = C2 (oxoglutarate); C3 (Glu,Arg,Pro), C4 (Lys) = C3 (oxoglutarate); C4 (Glu,Pro,Arg), C5 (Lys) = C4 (oxoglutarate); C5 (Glu,Pro,Arg), C6 (Lys) = C5 (oxoglutarate). ^{13}C abundance of ribose was calculated from C1' (adenosine, guanosine, cytidine) = C1 (ribose), C2' (adenosine, guanosine, cytidine) = C2 (ribose), C3' (adenosine, guanosine, cytidine) = C3 (ribose), C4' (adenosine, guanosine, cytidine) = C4 (ribose), C5' (adenosine, guanosine, cytidine) = C5 (ribose). Values are given \pm SD (standard deviation) with the number of available values for arithmetic mean value (*n*) in parentheses.

Metabolite	Position	^{13}C	<i>n</i>
		%	
Acetyl-CoA	1	5.3 \pm 1.3	(2)
	2	2.1 \pm 0.1	(2)
Pyruvate/phosphoenolpyruvate	1	5.7 \pm 2.3	(2)
	2	1.4 \pm 0.3	(5)
	3	1.9 \pm 0.2	(4)
Oxaloacetate	1	4.6 \pm 0.9	(2)
	2	1.8 \pm 0.4	(4)
	3	1.9 \pm 0.4	(4)
	4	5.3 \pm 1.3	(3)
2-Oxoglutarate	1	6.8	(1)
	2	2.2	(1)
	3	2.2	(1)
	4	2.2	(1)
	5	6.6	(1)
Ribose	1	2.6 \pm 0.5	(3)
	2	2.6 \pm 0.6	(3)
	3	5.4 \pm 0.9	(3)
	4	1.9 \pm 0.6	(3)
	5	2.1 \pm 0.3	(3)

The ^{13}C enrichments of C1, C2, and C3 of pyruvate were in close correspondence to C1, C2, and C3 of oxaloacetate, respectively. This excludes pyruvate formation by reductive carboxylation of acetyl-CoA. We suggest that pyruvate is synthesized from C1–C3 of malate or oxaloacetate. This is in contrast to the proposal of Kondratieva et al. [13] who suggested pyruvate formation via reductive carboxylation of acetyl-CoA. In summary, all labeling patterns are consistent with the proposed involvement of 3-hydroxypropionate in the novel carbon fixation cycle.

The incorporation of acetate labeled in position 1 or 2 is shown in Figs 9 and 10, respectively. Both experiments agree with the hypothesis that acetate can be introduced into the CO_2 fixation cycle as acetyl-CoA [2, 3, 13]. The label of [1- ^{13}C]acetate is redistributed to C2/C3 of the inherently sym-

Table 5. Averaged ^{13}C enrichments of central metabolic pools in *C. aurantiacus* grown with [1- ^{13}C]acetate. For details see Table 4.

Metabolite	Position	^{13}C	(<i>n</i>)
		%	
Acetyl-CoA	1	54.7 \pm 6.2	(6)
	2	8.1 \pm 0.9	(5)
Pyruvate/phosphoenolpyruvate	1	14.8 \pm 5.2	(4)
	2	18.8 \pm 3.4	(10)
	3	28.2 \pm 2.9	(8)
Oxaloacetate	1	15.8 \pm 6.2	(4)
	2	22.4 \pm 1.7	(8)
	3	21.1 \pm 2.6	(8)
	4	19.1 \pm 2.6	(6)
2-Oxoglutarate	1	17.3 \pm 1.9	(2)
	2	20.2 \pm 1.7	(4)
	3	21.7 \pm 0.3	(4)
	4	8.4 \pm 0.7	(4)
	5	53.3 \pm 7.3	(4)
Ribose	1	19.5 \pm 3.5	(3)
	2	16.0 \pm 3.4	(3)
	3	11.0 \pm 3.5	(3)
	4	16.5 \pm 3.0	(3)
	5	19.9 \pm 5.6	(3)

Table 6. Averaged ^{13}C enrichments of central metabolic pools in *C. aurantiacus* grown with [2- ^{13}C]acetate. For details see Table 4.

Metabolite	Position	^{13}C	(<i>n</i>)
		%	
Acetyl-CoA	1	2.9 \pm 0.4	(4)
	2	78.7 \pm 8.2	(6)
Pyruvate/phosphoenolpyruvate	1	4.9 \pm 0.4	(2)
	2	52.4 \pm 4.5	(10)
	3	39.5 \pm 4.1	(8)
Oxaloacetate	1	3.1 \pm 1.5	(2)
	2	51.5 \pm 8.4	(7)
	3	52.7 \pm 3.6	(7)
	4	4.0 \pm 2.7	(4)
2-Oxoglutarate	1	3.3	(1)
	2	52.8 \pm 4.7	(4)
	3	51.7 \pm 10.9	(4)
	4	82.1 \pm 8.2	(4)
	5	2.7 \pm 0.3	(3)
Ribose	1	30.4 \pm 1.4	(2)
	2	40.0 \pm 5.6	(2)
	3	6.9 \pm 0.1	(2)
	4	49.1 \pm 8.1	(2)
	5	31.6 \pm 7.6	(2)

metrical succinate molecule in the first round, indicated as closed circles in Fig. 9. Cleavage of malate yields [2- ^{13}C]acetyl-CoA and [2- ^{13}C]glyoxylate, indicated as asterisks in Fig. 9. If [2- ^{13}C]acetyl-CoA returns into the cycle, the label is again returned to C2/C3 of succinate. Following the same arguments, feeding of [2- ^{13}C]acetate should also introduce the isotope label exclusively to C2/C3 of succinate, irrespective of the number of rounds in the cycle (Fig. 10).

Precursor	[1- ¹³ C]Acetate	[2- ¹³ C]Acetate	[1- ¹³ C]3-Hydroxypropionate
Acetyl-CoA	$\boxed{55} \xrightleftharpoons[8]{2} \boxed{8}$	$\boxed{3} \xrightleftharpoons[2]{43} \boxed{79}$	$\boxed{5.3} - \boxed{2.1}$
Pyruvate	$\boxed{15} \xrightleftharpoons[2]{8} \boxed{19} \xrightleftharpoons[3]{3} \boxed{28}$	$\boxed{5} \xrightleftharpoons[3]{48} \boxed{52} \xrightleftharpoons[38]{24} \boxed{40}$	$\boxed{5.7} - \boxed{1.4} - \boxed{1.9}$
Oxaloacetate	$\boxed{16} \xrightleftharpoons[3]{4} \boxed{22} \xrightleftharpoons[6]{5} \boxed{21} \xrightleftharpoons[2]{2} \boxed{19}$	$\boxed{3} \xrightleftharpoons[3]{41} \boxed{52} \xrightleftharpoons[40]{39} \boxed{53} \xrightleftharpoons[46]{2} \boxed{4}$	$\boxed{4.6} - \boxed{1.8} - \boxed{1.8} - \boxed{5.3}$
2-Oxoglutarate	$\boxed{17} \xrightleftharpoons[3]{2} \boxed{20} \xrightarrow{7} \boxed{22} \xleftarrow[8]{5} \boxed{8} \xrightleftharpoons[2]{5} \boxed{58}$	$\boxed{3} \xrightleftharpoons[2]{45} \boxed{53} \xrightarrow{41} \boxed{52} \xleftarrow[56]{2} \boxed{82} \xrightleftharpoons[45]{2} \boxed{3}$	$\boxed{6.8} - \boxed{2.2} - \boxed{2.2} - \boxed{2.2} - \boxed{6.6}$
	C1 C2 C3 C4 C5	C1 C2 C3 C4 C5	C1 C2 C3 C4 C5

Fig. 7. ¹³C enrichment and ¹³C-¹³C coupling of central metabolites from the growth experiments with ¹³C-labeled acetates and 3-hydroxy[1-¹³C]propionate. Averaged ¹³C enrichments of individual carbons are shown inside the boxes. Fractions of ¹³C-¹³C coupled molecular species are shown between the boxes. A significant amount of multiple ¹³C-labeled molecular species is indicated by bold lines.

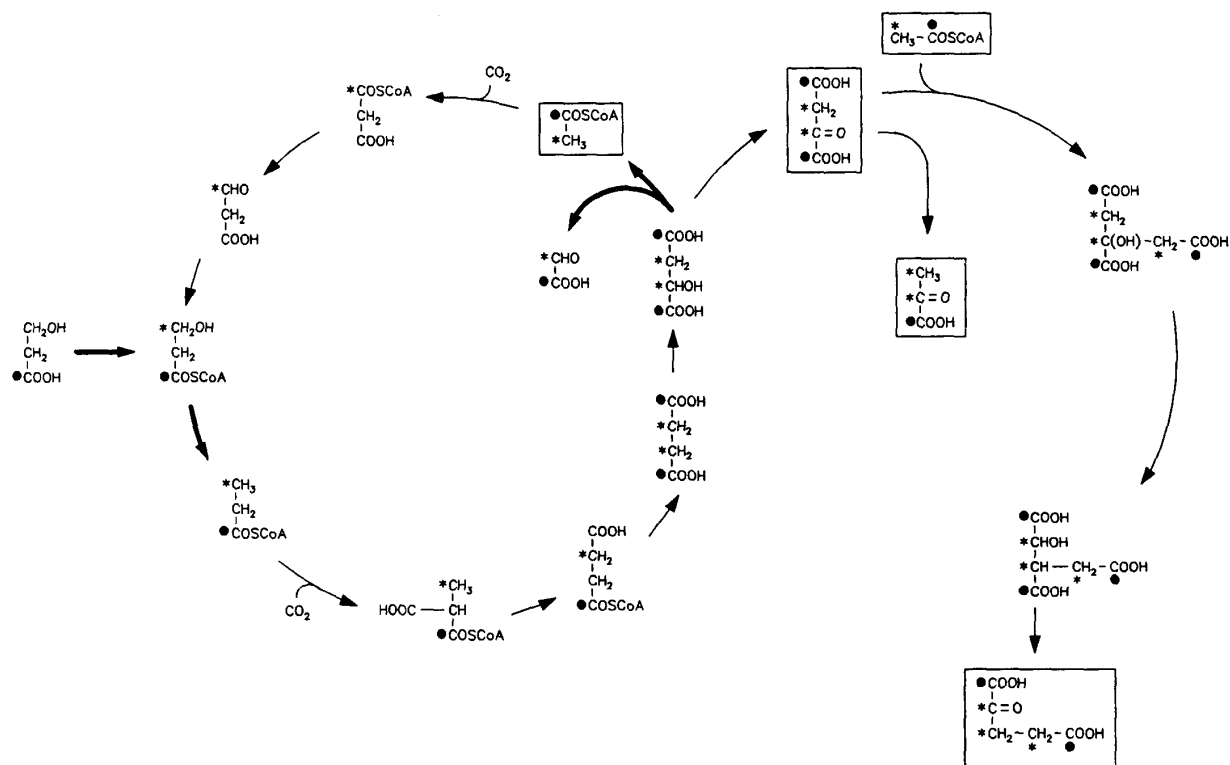


Fig. 8. Proposed scheme of carbon fixation in *C. aurantiacus* explaining the ¹³C enrichment patterns of central metabolites when 3-hydroxy[1-¹³C]propionate was added. Bold arrows illustrate key steps of carbon flow under the specific conditions of growth. Observed labeling and coupling patterns are indicated by boxes. ¹³C enrichment diverted by the first round (●) or subsequent rounds (*) of the autotrophic fixation cycle are indicated.

Based on the labeling patterns of the amino acids derived from succinate via oxaloacetate, it can be shown conclusively that the inner carbons of succinate are indeed labeled efficiently from both 1- and 2-labeled acetate. In this context, it should be noted that the reconstructed oxaloacetate labeling patterns does show the symmetrical label distribution expected on the basis of its origin from succinate.

The labeling patterns of C3–C5 in ribose were in good agreement to the labeling patterns of C1–C3 in pyruvate (Tables 4–6). These data suggest a conventional formation of ribose by condensation of two triose phosphates followed by decarboxylation of glucose 6-phosphate. In line with the

experimental data C3–C5 of ribose directly stem from C1–C3 of the triose phosphate/phosphoenolpyruvate pool by these mechanisms. Notably, the ¹³C-labeling and coupling patterns of glucose observed by Holo and Grace [14] after feeding of [1-¹³C]- or [2-¹³C]acetate to *C. aurantiacus* were quite similar to the labeling and coupling patterns of ribose and pyruvate in this study, confirming carbohydrate synthesis by gluconeogenesis.

Whereas the predictions based on the CO₂ fixation cycle are confirmed by the experimental data, two essential features of the experimentally determined labeling have yet to be explained. (a) The carbon fixation cycle should always

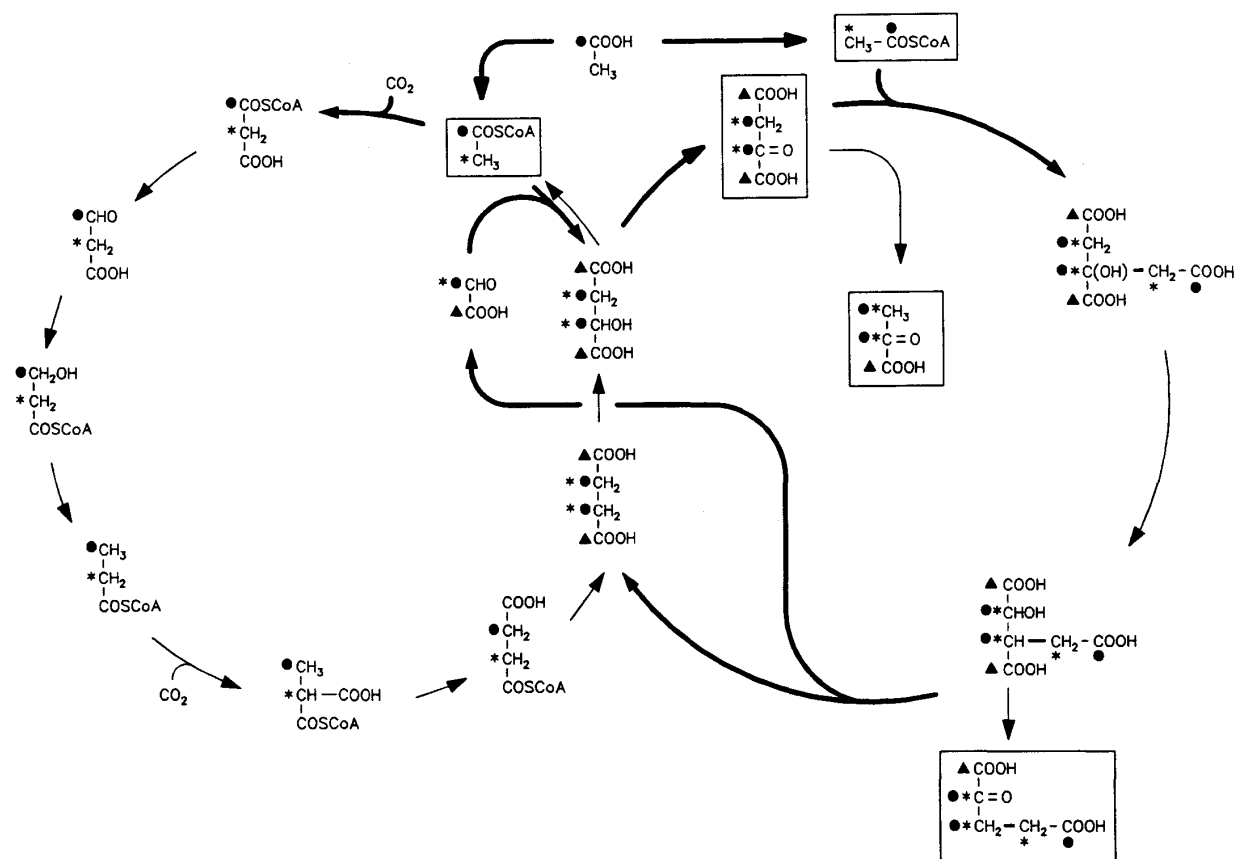


Fig. 9. Proposed scheme of carbon fixation in *C. aurantiacus* explaining the ¹³C enrichment and coupling patterns of central metabolites when [1-¹³C]acetate was added. ¹³C enrichment generated by key steps of the glyoxylate cycle are indicated by ▲. The presence of multiple ¹³C-labeled molecular species is indicated by bold bond lines. For other details see Fig. 8.

yield singly labeled oxaloacetate (i.e. [2/3-¹³C]₁oxaloacetate) irrespective of the number of rounds. However, a large amount of doubly labeled [2,3-¹³C]₂oxaloacetate was formed in the experiment with [2-¹³C]acetate (Figs 7 and 10). This species must necessarily be explained by condensation of two ¹³C-labeled organic molecules. (b) No isotope label can be delivered to the carboxyl groups of oxaloacetate by processing of 1- or 2-labeled acetate in the autotrophic carbon fixation cycle. Contrary to this expectation, the carboxyl groups of oxaloacetate were quite appreciably labeled from [1-¹³C]acetate (but not from [2-¹³C]acetate). Clearly, these data indicate the formation of oxaloacetate from acetate via a second pathway (Figs 9 and 10).

All experimental findings in the acetate incorporation experiments can be explained satisfactorily if we assume that a significant fraction of malate is formed by the standard glyoxylate cycle and not by the CO₂ fixation pathway. The key enzymes of the glyoxylate cycle in *C. aurantiacus* have been demonstrated [15]. As shown in Fig. 10, the condensation of [2-¹³C]acetyl-CoA (exogenous or regenerated in the carbon fixation cycle) with [2-¹³C]glyoxylate (product of the carbon fixation cycle or the glyoxylate cycle) yields malate and further oxaloacetate double labeled in C2 and C3. Moreover, the condensation of [2, 3-¹³C]₂oxaloacetate with [2-¹³C]acetyl-CoA yields isocitrate and further 2-oxoglutarate

labeled in C2, C3 and C4. Cleavage of this isocitrate species yields [2-¹³C]glyoxylate and [2, 3-¹³C]₂succinate. Passage of the [2, 3-¹³C]₂succinate through the glyoxylate cycle yield even more of the observed double-labeled oxaloacetate species. As described above, this species could not be explained on the basis of the CO₂ fixation cycle.

The same series of arguments explains the formation of [1, 4-¹³C]₂oxaloacetate in the experiment with [1-¹³C]acetate (Fig. 9). Briefly, [2/3-¹³C]₁oxaloacetate generated by the CO₂ fixation cycle can be condensed with [1-¹³C]acetyl-CoA resulting in the formation of isocitrate with label in position 1, 3, and 4. Cleavage of isocitrate leads then to carboxyl-labeled succinate and glyoxylate (indicated by ▲ in Fig. 9). Condensation of [1-¹³C]acetyl-CoA and [1-¹³C]glyoxylate yields [1, 4-¹³C]₂malate and further the observed [1, 4-¹³C]₂oxaloacetate. Cycling this species through the glyoxylate cycle yield multiply ¹³C-labeled 2-oxoglutarate, as shown in Fig. 9.

All enzymes required for the operation of the carbon fixation cycle have been identified in *C. aurantiacus* (unpublished results). However, enzymatic studies *in vitro* would be insufficient for a quantitative description of metabolite flux in the intact organism. This task can be solved by the *in vivo* studies described in the present paper. Under the experimental conditions, about two thirds of cell carbon is derived from CO₂. The remaining third was generated from the organi

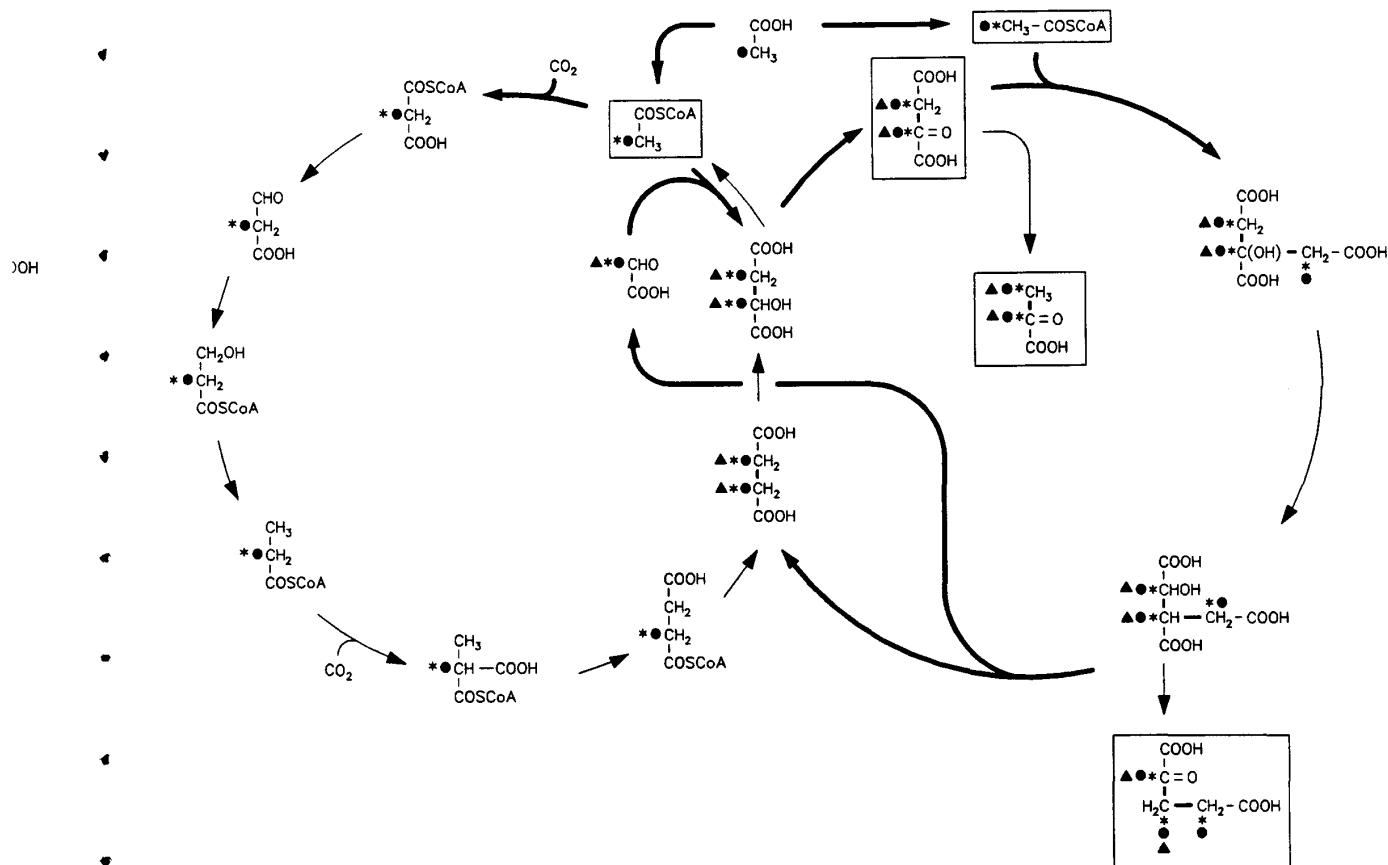


Fig. 10. Proposed scheme of carbon fixation in *C. aurantiacus* explaining the ^{13}C enrichment and coupling patterns of central metabolites when $[2-^{13}\text{C}]$ acetate was added. For details see Figs 8 and 9.

precursors, acetate or 3-hydroxypropionate. However, it is found that the metabolite flux is significantly different with acetate or 3-hydroxypropionate as organic nutrient.

The data show that incorporation of hydroxypropionate occurs essentially by the carbon fixation cycle. 2-Oxoglutarate is one of the end products of a metabolic side branch under these experimental conditions.

In contrast, acetate is metabolized in two different directions. Anterograde metabolism in the 3-hydroxypropionate cycle allows the fixation of CO_2 . Retrograde formation of malate from proffered acetate opens the way into the glyoxylate cycle. Succinate can now be formed under regeneration of glyoxylate which is required for sustained activity of the glyoxylate cycle.

We have no evidence for retrograde cycling of proffered 3-hydroxypropionate. The retrograde reaction may be thermodynamically unfavorable. However, it should be emphasized that the factors controlling the direction of metabolite flow in the fixation are as yet not known in any detail.

According to our hypothesis, the net product of CO_2 fixation is glyoxylate. This central intermediate must be channeled into the general metabolism. The pathway for glyoxylate utilization in *C. aurantiacus* remains to be determined.

Thanks are due to Ingrid König, Angelika Kohnle and Cornelia Krieger for secretarial work. We thank the *Deutsche Forschungs-*

gemeinschaft and the *Fonds der Chemischen Industrie* for financial support.

REFERENCES

- Fuchs, G. (1989) Alternative pathways of autotrophic CO_2 fixation, in *Autotrophic bacteria* (H. G. Schlegel, B. Bowien, eds) pp. 365–382, Science Tech. Publishers, Madison
- Holo, H. (1989) *Chloroflexus aurantiacus* secretes 3-hydroxypropionate, a possible intermediate in the assimilation of CO_2 and acetate, *Arch. Microbiol.* 151, 252–256.
- Strauß, G., Eisenreich, W., Bacher, A. & Fuchs, G. (1992) ^{13}C -NMR study of autotrophic CO_2 fixation pathways in the sulfur reducing Archaeobacterium *Thermoproteus neutrophilus* and in the phototrophic Eubacterium *Chloroflexus aurantiacus*. *Eur. J. Biochem.* 205, 853–866.
- Bauld, J. & Brock, D. (1973) Ecological studies of *Chloroflexis*, a gliding photosynthetic bacterium. *Arch. Microbiol.* 92, 267–284.
- Pierson, B. K. & Castenholz, R. W. (1974) A phototrophic gliding filamentous bacterium of hot springs, *Chloroflexus aurantiacus*, gen. and sp. nov. *Arch. Microbiol.* 100, 5–24.
- Erlenmeyer, E. (1878) Zur Geschichte der Aethylenmilchsäure, *Liebigs Ann. Chem.* 191, 261–285.
- Jacobs, W. A. & Heidelberger, M. (1917) The preparation of β -chloro and β -bromopropionic acids, *J. Am. Chem. Soc.* 39, 1465–1466.

8. Bax, A. & Davis, D. G. (1986) MLEV-17-based two-dimensional homonuclear magnetization transfer spectroscopy, *J. Magn. Reson.* 65, 355–360.
9. Bremser, W., Ernst, L., Franke, B., Gerhards, R. & Hardt, A. (1981) *Carbon-13 NMR spectra data*, Verlag Chemie, Weinheim.
10. Eisenreich W., Schwarzkopf B. & Bacher A. (1991) Biosynthesis of nucleotides, flavins, and deazaflavins in *Methanobacterium thermoautotrophicum*, *J. Biol. Chem.* 266, 9622–9631.
11. Fesik, S. W., Eaton, H. L., Olejniczak, E. T., Zuiderweg, E. R. P., McIntosh, L. P. & Dahlquist, F. W. (1990) 2D and 3D NMR spectroscopy employing ^{13}C - ^{13}C magnetization transfer by isotropic mixing. Spin system identification in large proteins, *J. Am. Chem. Soc.* 112, 886–888.
12. Klemme, J.-H., Laakmann-Ditges, G. & Mertschuweit, J. (1990) Cellular amino acid concentrations and regulation of aspartate-kinase in the thermophilic phototrophic prokaryote *Chloroflexus aurantiacus*, *Z. Naturforsch.* 45c, 74–78.
13. Kondratieva, E. N., Ivanovsky, R. N. & Krasilnikova, E. N. (1992) Carbon metabolism in *Chloroflexus aurantiacus*, *FEMS Microbiol. Lett.* 100, 269–272.
14. Holo, H. & Grace, D. (1987) Polyglucose synthesis in *Chloroflexus aurantiacus* studied by ^{13}C -NMR, *Arch. Microbiol.* 148, 292–297.
15. Løken, Ø. & Sirevag, R. (1982) Evidence for the presence of the glyoxylate cycle in *Chloroflexus*, *Arch. Microbiol.* 132, 276–279.